The Existence and Stability of Asymmetric Spike Patterns for the Schnakenberg Model

Michael J. Ward [1], Juncheng Wei[2]

Abstract

Asymmetric spike patterns are constructed for the two-component Schnakenburg reaction-diffusion system in the singularly perturbed limit of a small diffusivity of one of the components. For a pattern with k spikes, the construction yields k_1 spikes that have a common small amplitude and $k_2 = k - k_1$ spikes that have a common large amplitude. A k-spike asymmetric equilibrium solution is obtained from an arbitrary ordering of the small and large spikes on the domain. Explicit conditions for the existence and linear stability of these asymmetric spike patterns are determined using a combination of asymptotic techniques and spectral properties associated with a certain nonlocal eigenvalue problem. These asymmetric solutions are found to bifurcate from symmetric spike patterns at certain critical values of the parameters. Two interesting conclusions are that asymmetric patterns can exist for a reaction-diffusion system with spatially homogeneous coefficients under Neumann boundary conditions and that these solutions can be linearly stable on an $O(1)$ time scale.

1 Introduction

Over the past several decades there have been many different reaction-diffusion systems of activator-inhibitor type proposed to model various biological and chemical phenomena including, biological morphogenesis (cf. [3], [11], [4]), and the development of patterns on sea shells (cf. [12]). A review of recent progress in pattern formation is given in [10].

The usual first step in studying these reaction-diffusion models is to construct spatially homogeneous steady-state solutions. These solutions can occur when the coefficients in the reaction-diffusion equation are homogeneous in both space and time. A Turing-type stability analysis, originating from the work of Turing [15], is then used to analyze the stability of these spatially uniform steady-state solutions. This analysis leads to the determination of conditions for which spatially uniform steady-state solutions bifurcate to small amplitude spatially nonuniform solutions. The appeal of this type of analysis is that it is both widely applicable and is very simple.

However, many singularly perturbed reaction-diffusion systems admit steady-state solutions that locally have large spatial gradients. For example, spots and stripes occur in many sea shells

[1]Department of Mathematics, University of British Columbia, Vancouver, Canada V6T 1Z2
[2]Department of Mathematics, Chinese University of Hong Kong, Shatin, New Territories, Hong Kong

patterns. These patterns have been modeled by various reaction-diffusion systems involving various generalizations of the well-known Gierer-Meinhardt (GM) model [12]. A conventional Turing-type stability analysis is not applicable for studying the stability of these solutions. A fundamental issue is how should the Turing-type stability analysis be modified in order to study the stability of localized solutions for reaction-diffusion systems.

A second feature of interest is that it is commonly believed that reaction-diffusion systems with spatially homogeneous coefficients under Neumann boundary conditions typically only admit solutions that obey certain symmetry conditions. In contrast, biological patterns in nature can have some inherent asymmetry. In recent years there has been a focus on investigating various mechanisms that give rise to asymmetric patterns in reaction-diffusion models. The mechanisms that have been considered include the effect of Robin-type boundary conditions [13], the effect of spatially varying diffusion coefficients [9], and the effect of precursor gradients modeled by spatially varying coefficients in the differential operator [5]. An interesting question is whether asymmetric steady-state patterns can exist for such systems without these mechanisms.

The goal of this paper is to continue the investigation, initiated for the GM model in [6], [16], [18], and [2], of the construction and stability of localized symmetric and asymmetric spike patterns for spatially uniform reaction-diffusion systems under homogeneous Neumann boundary conditions. In [6] a generalization of a Turing-type stability analysis was used to determine the stability of symmetric spike patterns for the one-dimensional GM model. In [16] and [18] asymmetric steady-state patterns for the GM model were constructed and the stability of these solutions was investigated. A different approach for the construction of asymmetric patterns was given in [2]. The dynamics of asymmetric spike patterns was analyzed in [8].

Our goal is to show that the mathematical analyses used to construct symmetric and asymmetric spike patterns for the GM model and to determine the stability of these solutions is easily adapted to other reaction-diffusion systems. More specifically, in this paper we use a formal asymptotic analysis to study the existence and stability of asymmetric equilibrium spike patterns for the well-known Schnakenburg model [14]. In a certain parameter regime the Schakenburg model is one of the simplest models that can be analyzed explicitly to show the occurrence of Hopf bifurcations generating periodic patterns. In other parameter regimes it yields spike-type equilibrium patterns.

The Schnakenburg model is given by

$$u_t = D_1 u_{xx} - u + vu^2\,, \qquad -1 < x < 1\,, \quad t > 0\,, \tag{1.1a}$$

$$v_t = D_2 v_{xx} + B - vu^2\,, \qquad -1 < x < 1\,, \quad t > 0\,, \tag{1.1b}$$

$$u_x(\pm 1, t) = v_x(\pm 1, t) = 0\,, \tag{1.1c}$$

where $D_1 > 0$, $D_2 > 0$ and $B > 0$ are constants. We introduce new variables by

$$u = \hat{u}/(2B)\,, \qquad v = 2B\hat{v}\,. \tag{1.2}$$

Substituting (1.2) into (1.1), and dropping the hat notation, we obtain

$$u_t = D_1 u_{xx} - u + vu^2\,, \qquad -1 < x < 1\,, \quad t > 0\,, \tag{1.3a}$$

$$v_t = D_2 v_{xx} + \frac{1}{2} - bvu^2\,, \qquad -1 < x < 1\,, \quad t > 0\,, \tag{1.3b}$$

$$u_x(\pm 1, t) = v_x(\pm 1, t) = 0\,, \tag{1.3c}$$

where $b^{-1} = 4B^2$. To find a scaling appropriate for spike solutions we assume that u diffuses more slowly than v, so that

$$D_1 = \varepsilon^2\,, \qquad D_2 = D\,, \tag{1.4}$$

where $\varepsilon \ll 1$. We then introduce the new variables

$$D = \frac{\tilde{D}}{\varepsilon}\,, \qquad v = \varepsilon\tilde{v}\,, \qquad u = \frac{\tilde{u}}{\varepsilon}\,. \tag{1.5}$$

Substituting (1.5) into (1.1), and dropping the tilde variables, we obtain the following singularly perturbed reaction-diffusion system of interest:

$$u_t = \varepsilon^2 u_{xx} - u + vu^2\,, \qquad -1 < x < 1\,, \quad t > 0\,, \tag{1.6a}$$

$$\varepsilon v_t = D v_{xx} + \frac{1}{2} - \frac{b}{\varepsilon} vu^2\,, \qquad -1 < x < 1\,, \quad t > 0\,, \tag{1.6b}$$

$$u_x(\pm 1, t) = v_x(\pm 1, t) = 0\,. \tag{1.6c}$$

The asymmetric equilibrium solutions to (1.6) that we construct in the limit $\varepsilon \to 0$ have the form of a sequence of spikes of different heights. Specifically, for a pattern with k spikes, our asymptotic analysis yields $k_1 > 0$ spikes that have a common small amplitude and $k_2 = k - k_1 > 0$ spikes that have a common large amplitude. A k-spike asymmetric equilibrium solution is obtained from an arbitrary ordering of the small and large spikes across the interval. An example of such a spike pattern that is obtained from the analysis is shown in Fig. 1(a) and Fig. 1(b). Such solutions are shown to exist when D is less than some critical value D_m that depends on k_1, k_2, and b. For some range of parameters it is also shown that solution multiplicity occurs in the sense that there are two possible solutions with k_1 small and k_2 large spikes. At a specific parameter value, an

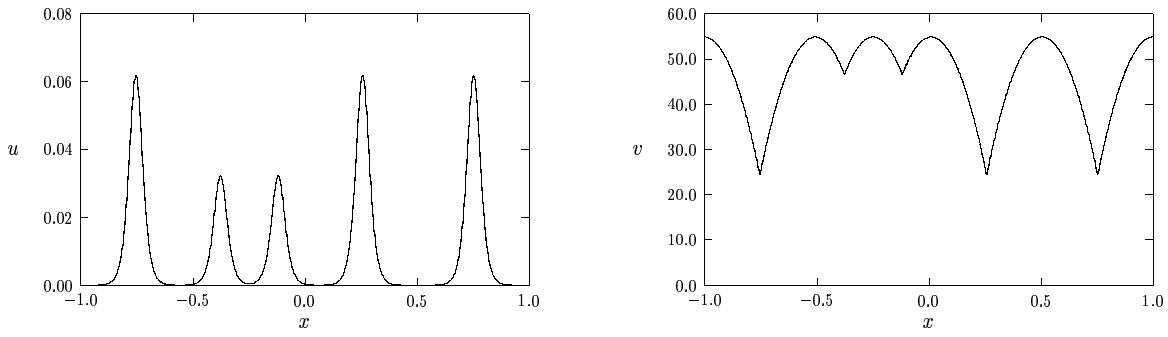

(a) u versus x (b) v versus x

Figure 1: Plots of u and v versus x for a five-spike asymptotic asymmetric equilibrium solution of the form BAABB for $D = 0.0005$, $b = 1$ and $\varepsilon = 0.02$. This solution is unstable.

asymmetric solution branch with k spikes is shown to to bifurcate from the symmetric branch s_k for which k spikes have an equal amplitude.

Next, we analyze the linear stability of these asymmetric equilibrium spike patterns. There are two classes of eigenvalues to be considered: the large $O(1)$ eigenvalues and the small $O(\varepsilon^2)$ eigenvalues. For the large eigenvalues, in Section 3 we obtain an explicit stability criterion for the asymmetric spike patterns in terms of the maximum eigenvalue of a certain matrix eigenvalue problem. We show that, with respect to the large $O(1)$ eigenvalues, the asymmetric spike solutions are stable when $D > D_e$, where the critical value D_e depends on k_1, k_2, b, and on the specific orientation of the small and large spikes within a given k-spike sequence. The stability of the k-spike patterns with respect to the small eigenvalues of order $O(\varepsilon^2)$ is also studied. We derive a generalized matrix eigenvalue problem that determines the small eigenvalues. An asymmetric k-spike pattern is shown to bifurcate from the symmetric branch s_k at the parameter value where $k-1$ small eigenvalues simultaneously cross through zero. From numerical computations of the generalized matrix eigenvalue problem, we show that these bifurcating asymmetric branches are all unstable with respect to the small eigenvalues. Our main conclusion is that, although all of these asymmetric patterns are ultimately unstable, there are ranges of D for which asymmetric equilibria will persist for long time intervals of the order $t << O(\varepsilon^{-2})$.

The outline of this paper is as follows. In §2 we use the method of matched asymptotic ex-

pansions to construct a k-spike asymmetric equilibrium spike solution to (1.6). In §3 we determine conditions that ensure that the large $O(1)$ eigenvalues associated with the linearization of (1.6) about the asymmetric equilibrium solution have negative real parts. When this condition holds, we say that the pattern is stable with respect to the large $O(1)$ eigenvalues. Examples of the theory for solutions with fewer than five spikes, together with some specific results for these solutions, are given in §4. In §5 we analyze the small eigenvalues and we calculate their algebraic sign numerically for the specific examples discussed in §4. Some concluding remarks are made in §6.

2 Asymmetric Equilibrium Solutions

In the limit $\varepsilon \to 0$, we construct an asymmetric k-spike equilibrium solution to (1.6) in the form of a sequence of spikes of different heights. To do so, we first must construct a local *canonical* one-spike equilibrium solution to (1.6) on a finite domain of length $2l$, where $l > 0$ is a parameter. This problem is shown to have two different solutions. A k-spike asymmetric solution is then obtained by using translates of these two local solutions in such a way to ensure that the resulting equilibrium solution to (1.6) on the interval $-1 \le x \le 1$ is C^1 continuous.

The local one-spike solution $u = u(x)$ and $v = v(x)$, with the spike centered at $x = 0$, satisfies

$$\varepsilon^2 u_{xx} - u + vu^2 = 0\,, \qquad -l < x < l\,, \tag{2.1a}$$

$$Dv_{xx} + \frac{1}{2} - \frac{b}{\varepsilon} vu^2 = 0\,, \qquad -l < x < l\,, \tag{2.1b}$$

$$v_x(\pm l) = u_x(\pm l) = 0\,, \tag{2.1c}$$

where the functions u and v are even functions of x. In the limit $\varepsilon \to 0$, $u(l)$ is exponentially small and $v(l) = O(1)$. For $\varepsilon \to 0$, the asymptotic solution to (2.1) is readily obtained by the method of matched asymptotic expansions. We calculate that

$$u(x) \sim \frac{1}{v(0)} u_c(x/\varepsilon)\,, \tag{2.2}$$

where $u_c(y)$ is the unique solution to

$$u_c'' - u_c + u_c^2 = 0\,, \qquad -\infty < y < \infty\,, \tag{2.3a}$$

$$u_c \to 0 \quad \text{as} \quad |y| \to \infty\,; \qquad u_c'(0) = 0\,, \qquad u_c(0) > 0\,. \tag{2.3b}$$

The solution to (2.3) is

$$u_c(y) = \frac{3}{2} \operatorname{sech}^2(y/2)\,. \tag{2.4}$$

Since u is localized near $x = 0$, the term $\varepsilon^{-1} bvu^2$ in (2.1b) can be asymptotically approximated as a multiple of a Dirac mass. Thus, when $\varepsilon \ll 1$, the problem for $v(x)$ is

$$Dv'' + \frac{1}{2} - \frac{ba}{v(0)}\delta(x) = 0\,, \qquad -l < x < l\,, \tag{2.5a}$$

$$v'(\pm l) = 0\,. \tag{2.5b}$$

Here $\delta(x)$ is the delta function and a is defined by

$$a = \int_{-\infty}^{\infty} [u_c(y)]^2 \, dy = \frac{9}{4}\int_{-\infty}^{\infty} \operatorname{sech}^4(y/2) \, dy = 6\,. \tag{2.5c}$$

The solvability condition for (2.5) is obtained by integrating (2.5a) across the interval. This yields,

$$v(0) = \frac{6b}{l}\,. \tag{2.6a}$$

Then, the solution to (2.5) is written as

$$v(x) = lG_l(x;0)\,, \tag{2.6b}$$

where $G_l(x;0)$ is the modified Green's function satisfying

$$DG_{lxx} + \frac{1}{2l} - \delta(x) = 0\,, \qquad -l < x < l\,, \tag{2.7a}$$

$$G_{lx}(\pm l;0) = 0\,, \tag{2.7b}$$

$$G_l(0;0) = \frac{v(0)}{l} = \frac{6b}{l^2}\,. \tag{2.7c}$$

A simple calculation gives,

$$G_l(x;0) = -\frac{x^2}{4lD} + E - \frac{1}{2D}\left(l - |x|\right)\,, \quad -l \le x \le l\,, \tag{2.8a}$$

where the constant E is given by

$$E = \frac{l}{2D} + \frac{6b}{l^2}\,. \tag{2.8b}$$

In terms of this solution, we calculate $v(l) = lG_l(l;0)$ explicitly as

$$v(l) = \frac{l^2}{4D} + \frac{6b}{l}\,. \tag{2.9}$$

The next step is to determine all different values of l, labeled by l_1,..,l_n, such that $v(l_1) =, .., = v(l_n)$. For a certain range of parameters, as shown below, there are exactly two such values of l. These local canonical solutions corresponding to different values of l are then used to obtain a global asymmetric spike pattern for (1.6) on the interval $-1 < x < 1$.

It is convenient to write $v(l)$ in the form

$$v(l) = \frac{q^2}{4D} \left[\beta \left(l/q\right)\right]^{-1} , \qquad q \equiv \left[24bD\right]^{1/3} , \tag{2.10a}$$

where the function $\beta(z)$ is defined by

$$\beta(z) \equiv \left[z^2 + 1/z\right]^{-1} . \tag{2.10b}$$

The function $\beta(z) > 0$ in (2.10b) has several key properties. It has a unique global maximum point at $z = z_c$, where

$$z_c = 2^{-1/3} . \tag{2.11}$$

In addition, $\beta^{'}(z) > 0$ on $[0, z_c)$ and $\beta^{'}(z) < 0$ on (z_c, ∞). Therefore, given any $z \in (0, z_c)$, there exists a unique point $\tilde{z} \in (z_c, \infty)$ such that $\beta(z) = \beta(\tilde{z}) \equiv \beta[f(z)]$. The inverse function $\tilde{z} = f(z)$ is readily calculated from the explicit form of $\beta(z)$ given in (2.10b). This leads to the first result.
Result 2.1: *On the interval $z \in (0, z_c]$, the inverse function is*

$$\tilde{z} = f(z) = -\frac{z}{2} + \frac{\sqrt{z^2 + 4/z}}{2} . \tag{2.12}$$

Some key properties of the function $f(z)$ on $z \in (0, z_c]$, which are needed below are: $f(z_c) = z_c$, $f(z)$ is convex on $(0, z_c)$, and $f^{'}(z) < -1$ on $(0, z_c)$ with $f^{'}(z_c) = -1$. In Fig. 2 and Fig. 2 we plot $\beta(z)$ and the inverse function $f(z)$, respectively.

The implication of these results for $\beta(z)$ and $f(z)$, obtained from examining (2.10a), is that there are exactly two different types of spikes. We summarize this result as follows.
Result 2.2: *Given any l, with $l/q < z_c$, there exists a unique $\tilde{l}$, with $\tilde{l}/q \equiv \tilde{z} > z_c$, such that $v(l) = v(\tilde{l})$.*

We refer to solutions of length l and $\tilde{l}$ as A-type and B-type spikes, respectively. From (2.6a) and (2.2) we conclude that $v(0)$ is a decreasing function of l and $u(0)$ is an increasing function of l. Thus, the maximum value of u associated with an A-type spike is smaller than that for a B-type spike. Consequently, we refer to A-type and B-type spikes as small and large spikes, respectively.

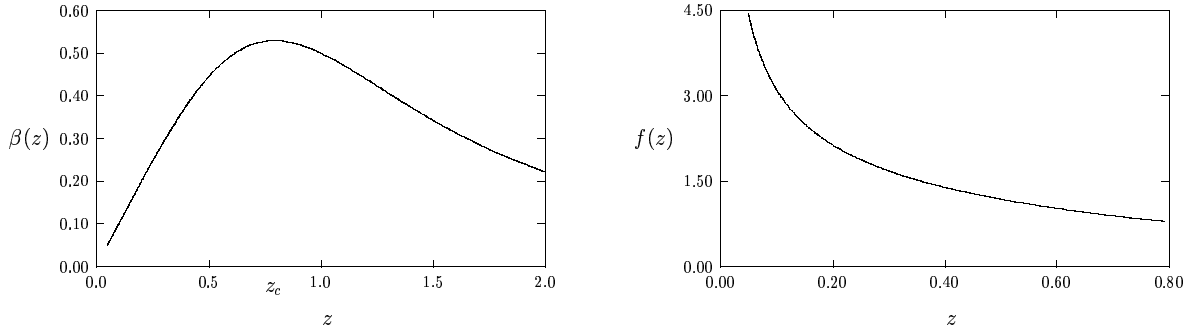

Figure 2: Plots of the functions $\beta(z)$ and $f(z)$

We now construct a k-spike equilibrium solution to (1.6) on $-1 \le x \le 1$ with $k_1 \ge 0$ spikes of type A and $k_2 = k - k_1 \ge 0$ spikes of type B. The spikes are arranged in any particular order from left to right across the interval as

$$\text{ABAAB....B}\,, \qquad k_1 - \text{A's}\,, \qquad \text{and} \qquad k_2 - \text{B's}\,. \tag{2.13}$$

In the construction of these patterns we use translation invariance and the fact that $v(l) = v(\tilde{l})$. This allows us to glue A and B type spikes together to satisfy a C^1 continuity for the global function v defined on $[-1, 1]$. Since the support of an A-spike and a B-spike is $2l$ and $2\tilde{l}$, respectively, we must impose the length constraint $2k_1 l + 2k_2\tilde{l} = 2$. In addition, we must impose that $\beta(l/q) = \beta(\tilde{l}/q)$, which ensures that v is C^1 continuous. We summarize this construction of asymmetric spike patterns in the next result.

Result 2.3: *Let k_1 and k_2 be non-negative integers such that $k_1 + k_2 = k$. Let z with $z \in (0, z_c]$ and $\tilde{z} \in [z_c, \infty)$ be solutions to the nonlinear algebraic system*

$$k_1 z + k_2 \tilde{z} = \frac{1}{q}\,, \tag{2.14a}$$

$$\beta(z) = \beta(\tilde{z})\,. \tag{2.14b}$$

Then, defining l and $\tilde{l}$ by $l = qz$ and $\tilde{l} = q\tilde{z}$, we obtain a spike pattern with k_1 small spikes each having support $2l$ and k_2 large spikes each having support $2\tilde{l}$. Here q is defined in terms of D in (2.10a).

We now investigate the solvability of the system (2.14). The solution to (2.14b) is simply $\tilde{z} = f(z)$. Thus, the solutions to (2.14) are determined by the intersection points of the curve

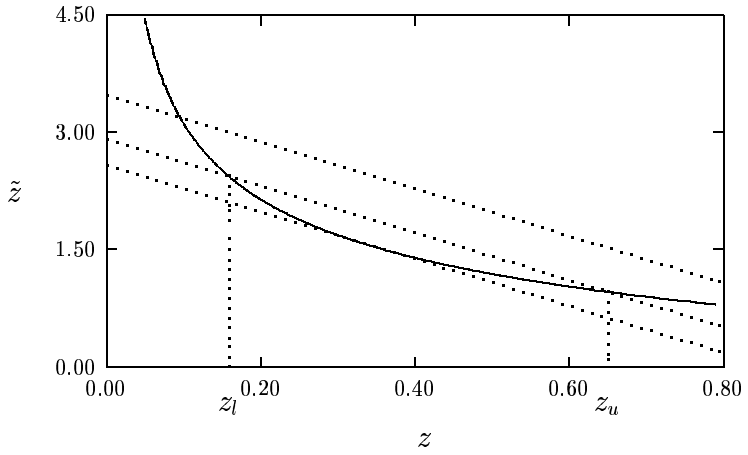

Figure 3: Graphical plot of (2.14) when $k_1 = 3$, $k_2 = 1$ and $b = 1$. The solid curve is $\tilde{z} = f(z)$. The dotted straight line (2.14a) is plotted for $D = D_{m_1} = 0.002445$, $D = 0.0017$ and $D = 0.0010$. When $D = 0.002445$ this line is tangent to $f(z)$. When $D = 0.0017$ there are two solutions z_l and z_u to (2.14), and only one solution when $D = 0.0010$.

$\tilde{z} = f(z)$ with the straight line $\tilde{z} = -k_1 z/k_2 + 1/(qk_2)$ on the interval $0 < z \leq z_c$. From the properties of $f(z)$ listed following (2.12) above, it is clear that there are two different cases to consider:

$$\text{Case 1:} \quad k_1/k_2 \leq 1\,; \qquad \text{Case 2:} \quad k_1/k_2 > 1\,. \tag{2.15}$$

Since $f(z)$ is convex and $f'(z) \leq -1$ on $z \in (0, z_c]$, with equality only when $z = z_c$, we can readily obtain the following result:

Result 2.4 (Case 1): *Let $k_1/k_2 \leq 1$. Then, when $D < D_m$, there exists a unique solution $(z, \tilde{z})$ to (2.14) on $z \in (0, z_c)$ and $\tilde{z} \in (z_c, \infty)$. The critical value D_m is*

$$D_m = \left[12bk^3\right]^{-1}\,, \qquad k = k_1 + k_2\,. \tag{2.16a}$$

When $D = D_m$, then $z = \tilde{z} = z_c$ and hence $l = \tilde{l} = 1/k$. In this special case, we get a symmetric k-spike solution with spikes of equal height. The numerical values for D_m are

$$D_m = 0.0104/b \quad (k = 2); \qquad D_m = 0.00308/b \quad (k = 3); \qquad D_m = 0.00130/b \quad (k = 4)\,. \tag{2.16b}$$

The solvability of (2.14) is more complicated when there are more small than large spikes on the interval (i. e. when $k_1/k_2 > 1$). In this case, which we show graphically in the $\tilde{z}$, z plane of Fig. 3, as D is decreased from a large value the straight line of slope $-k_1/k_2$ first intersects the curve $\tilde{z} = f(z)$ at a point of tangency at some critical value of D, labeled by D_{m_1}. As D is decreased slightly below D_{m_1}, there are exactly two roots to (2.14) until D is decreased to the value D_m defined in (2.16a). When D is decreased below D_m there is only one solution to (2.14) on $(0, z_c)$.

Result 2.5 (Case 2): *Let $k_1/k_2 > 1$. Then, there exists a critical value $D_{m_1} > D_m$ such that the solution multiplicity property for (2.14) on the interval $z \in (0, z_c)$ and $\tilde{z} \in (z_c, \infty)$ is as follows:*

$$\begin{aligned} &\text{If } \ D > D_{m_1} \qquad \rightarrow \quad \textit{there are no solutions}\,, \\ &\text{If } \ D_m < D < D_{m_1} \qquad \rightarrow \quad \textit{there are exactly two solutions}\,, \\ &\text{If } \ D < D_m \qquad \rightarrow \quad \textit{there is exactly one solution}\,. \end{aligned} \tag{2.17a}$$

The critical value D_{m_1} is the solution of the tangency condition system

$$k_1 z + k_2 f(z) = \frac{1}{q}\,, \qquad f^{'}(z) = -k_1/k_2. \tag{2.17b}$$

By using (2.12) for $f(z)$ we can calculate D_{m_1} explicitly. The condition $f^{'}(z) = -k_1/k_2$ yields the quadratic equation for z^3 given by

$$(z^3 - 2)^2 = \gamma^2 z^3 (z^3 + 4)\,, \qquad \text{where} \qquad \gamma = 1 - \frac{2k_1}{k_2}\,. \tag{2.18}$$

The solution to (2.18) on $(0, z_c)$ is

$$z_* = \left[\frac{2(1+\gamma^2) - 2\sqrt{(1+\gamma^2)^2 - (1-\gamma^2)}}{(1-\gamma^2)} \right]^{1/3}\,. \tag{2.19}$$

Finally, from $k_1 z + k_2 f(z) = 1/q$, and the definition of q in (2.10a), we obtain that

$$D_{m_1} = \frac{1}{24b} \left[k_2 f(z_*) + k_1 z_* \right]^{-3}\,. \tag{2.20}$$

Numerical values for D_{m_1} calculated from (2.20) are

$$D_{m_1} = 0.004009/b \quad (k_1 = 2,\ k_2 = 1); \qquad D_{m_1} = 0.002445/b \quad (k_1 = 3,\ k_2 = 1)\,. \tag{2.21}$$

To summarize, consider a particular fixed ordering of small and large spikes across the interval. When $D < D_m$, and when there are more large B-spikes than small A-spikes, there is exactly one

asymmetric pattern with that particular ordered sequence. However, when there are more small than large spikes in the sequence, then for some range of D there are exactly two such patterns that have the same ordering.

Finally, we calculate the equilibrium solution $u = u_e$ and $v = v_e$ on $-1 < x < 1$. Given a specific ordered sequence of large and small spikes on the interval, we have from (2.6a) that $v_e(x_j) \equiv v_j = 6b/l_j$, where $l_j = l$ if the $j^{\rm th}$ spike is A-type and $l_j = \tilde{l}$ if the $j^{\rm th}$ spike is B-type. Near the j^{th} spike, $u_e \sim v_j^{-1} u_c\left[\varepsilon^{-1}(x - x_j)\right]$. Therefore, (1.6b) for v_e becomes

$$Dv_{exx} + \frac{1}{2} - 6b\sum_{j=1}^{k} \frac{1}{v_j}\delta(x - x_j) = 0\,, \qquad -1 < x < 1\,, \tag{2.22a}$$

$$v_{ex}(\pm 1) = 0\,. \tag{2.22b}$$

The solvability condition for (2.22) is $\sum_{j=1}^{k} v_j^{-1} = (6b)^{-1}$. This condition is equivalent to $k_1 l + k_2 \tilde{l} = 1$, which is satisfied by (2.14a). The solution to (2.22) is then readily represented in terms of an appropriate Green's function. In this way, we obtain the following main result.

Proposition 2.1 (Asymmetric): *Let $\varepsilon \to 0$ and fix a particular ordering of small and large spikes across the interval as in (2.13). Then, for $D < D_m$, there exists an asymmetric k-spike equilibrium solution (u_e, v_e) to (1.6) of the form,*

$$u_e(x) \sim \sum_{j=1}^{k} v_j^{-1} u_c\left[\varepsilon^{-1}(x - x_j)\right]\,. \tag{2.23a}$$

The constant v_j, given by $v_j = v_e(x_j)$ satisfies

$$v_j = 6b/l_j\,, \qquad j = 1, .., k\,. \tag{2.23b}$$

Here for each j, $l_j = l$ or $l_j = \tilde{l}$ depending on whether the j^{th} spike is A-type or B-type, respectively. Here l and $\tilde{l}$ are determined in terms of k_1, k_2 and q by (2.14). The value $l_j = l$ must occur $k_1 > 0$ times, while $l_j = \tilde{l}$ must occur $k_2 = k - k_1 > 0$ times. The function v_e is

$$v_e(x) \sim \sum_{j=1}^{k} \frac{6b}{v_j} G(x; x_j) + \bar{v}\,, \tag{2.24a}$$

where $G(x; x_j)$ satisfies

$$DG_{xx} + \frac{1}{2} = \delta(x - x_j)\,, \qquad -1 < x < 1\,, \tag{2.25a}$$

$$G_x(\pm 1; x_j) = 0\,, \qquad \int_{-1}^{1} G(x; x_j)\, dx = 0\,. \tag{2.25b}$$

The solution is

$$G(x;x_j) = -\frac{1}{4D}\left(x^2 + x_j^2\right) + \frac{1}{2D}|x - x_j| - \frac{1}{6D}\,. \tag{2.25c}$$

The constant $\bar{v}$ in (2.24a), given by $\bar{v} = \frac{1}{2}\int_{-1}^{1} v_e\,dx$, is calculated from

$$\bar{v} = v_i - 6b\sum_{j=1}^{k} G(x_i;x_j)/v_j\,, \tag{2.26}$$

where the right-hand side in (2.26) is independent of i. The spike locations x_j satisfy

$$x_1 = l_1 - 1\,, \qquad x_k = 1 - l_k\,, \qquad x_{j+1} = x_j + l_{j+1} + l_j\,, \quad j = 1,..,k-2\,. \tag{2.27}$$

When $k_1/k_2 > 1$ and $D_m < D < D_{m_1}$, this result still holds. However, as discussed in Result 2.5 above, there are two possible values of the pair l and $\tilde{l}$ for each D on this range. Examples of the theory are given in §4.

3 The Stability Analysis: Large Eigenvalues

To study the stability of the asymmetric solutions u_e and v_e constructed in §2, we substitute

$$u(x,t) = u_e(x) + e^{\lambda t}\phi(x)\,, \qquad v(x,t) = v_e(x) + e^{\lambda t}\eta(x)\,, \tag{3.1}$$

into (1.6) where $\eta \ll 1$ and $\phi \ll 1$. This leads to the eigenvalue problem

$$\varepsilon^2\phi_{xx} - \phi + 2v_e u_e\phi + u_e^2\eta = \lambda\phi\,, \qquad -1 < x < 1\,, \tag{3.2a}$$

$$D\eta_{xx} - \frac{b}{\varepsilon}u_e^2\eta = \frac{2b}{\varepsilon}v_e u_e\phi + \varepsilon\lambda\eta\,, \qquad -1 < x < 1\,, \tag{3.2b}$$

$$\phi_x(\pm 1) = \eta_x(\pm 1) = 0\,. \tag{3.2c}$$

The spectrum of (3.2) contains large eigenvalues that are $O(1)$ as $\varepsilon \to 0$ and small eigenvalues that are $O(\varepsilon^2)$ as $\varepsilon \to 0$. The goal is to determine the conditions under which both sets of eigenvalues have negative real parts. In this section we analyze the large eigenvalues and in §5 we study the small eigenvalues.

To examine the large eigenvalues, we look for an eigenfunction of (3.2) in the form

$$\phi(x) \sim \sum_{j=1}^{k} \phi_j\left[\varepsilon^{-1}(x - x_j)\right]\,, \tag{3.3}$$

where $\phi_j(y) \to 0$ exponentially as $|y| \to \infty$. Since both u_e and ϕ are localized near each x_j as $\varepsilon \to 0$, the coefficients in the differential operator of (3.2b) are multiples of Dirac masses. Letting $\varepsilon \to 0$, labeling $v_e(x_j) = v_j$, and assuming that $\lambda = O(1)$ as $\varepsilon \to 0$, we obtain that (3.2b) reduces asymptotically to

$$D\eta_{xx} - \left[6b \sum_{j=1}^{k} \frac{1}{v_j^2} \delta(x - x_j) \right] \eta = 2b \sum_{j=1}^{k} \int_{-\infty}^{\infty} u_c \phi_j \, dy \; \delta(x - x_j) \,. \tag{3.4}$$

This problem is equivalent to

$$D\eta_{xx} = 0 \qquad -1 < x < 1 \,; \qquad \eta_x(\pm 1) = 0 \,, \tag{3.5a}$$

$$[\eta]_j = 0 \,; \qquad [D\eta_x]_j = \frac{6b}{v_j^2} \eta(x_j) + 2b \int_{-\infty}^{\infty} u_c \phi_j \, dy \,, \qquad j = 1, .., k \,. \tag{3.5b}$$

Here we have defined $[v]_j = v(x_{j^+}) - v(x_{j^-})$.

In the analysis below we need to calculate $\eta(x_j)$ from (3.5). By solving (3.5) on each subinterval as done in Appendix A, we can readily derive a linear system for $\eta(x_j)$ for $j = 1, .., k$ in the form

$$(\mathcal{B} + \mathcal{C}) \, \boldsymbol{\eta} = \boldsymbol{\omega} \,, \tag{3.6}$$

where $\mathcal{B}$, $\mathcal{C}$, $\boldsymbol{\eta}$, and $\boldsymbol{\omega}$ are defined by

$$\mathcal{C} \equiv \frac{6b}{D} \begin{pmatrix} 1/v_1^2 & 0 & \cdots & 0 \\ 0 & \ddots & \cdots & 0 \\ \vdots & \vdots & \ddots & \vdots \\ 0 & 0 & \cdots & 1/v_k^2 \end{pmatrix} , \quad \boldsymbol{\eta} \equiv \begin{pmatrix} \eta(x_1) \\ \vdots \\ \eta(x_k) \end{pmatrix} , \quad \boldsymbol{\phi} \equiv \begin{pmatrix} \phi_1 \\ \vdots \\ \phi_k \end{pmatrix} , \quad \boldsymbol{\omega} = -\frac{2b}{D} \int_{-\infty}^{\infty} u_c \boldsymbol{\phi} \, dy \,, \tag{3.7a}$$

and

$$\mathcal{B} \equiv \begin{pmatrix} 1/d_2 & -1/d_2 & 0 & \cdots & 0 & 0 & 0 \\ -1/d_2 & 1/d_2 + 1/d_3 & \ddots & \ddots & \ddots & 0 & 0 \\ 0 & \ddots & \ddots & \ddots & \ddots & \ddots & 0 \\ \vdots & \ddots & \ddots & \ddots & \ddots & \ddots & \vdots \\ 0 & \ddots & \ddots & \ddots & \ddots & \ddots & 0 \\ 0 & 0 & \ddots & \ddots & \ddots & 1/d_{k-1} + 1/d_k & -1/d_k \\ 0 & 0 & 0 & \cdots & 0 & -1/d_k & 1/d_k \end{pmatrix} . \tag{3.7b}$$

In (3.7b) we have defined the inter-spike distances as

$$d_j = x_j - x_{j-1}\,, \qquad j = 2, .., k\,. \tag{3.7c}$$

Since the matrix $\mathcal{B} + \mathcal{C}$ is symmetric and invertible, we obtain that

$$\boldsymbol{\eta} = (\mathcal{B} + \mathcal{C})^{-1}\,\boldsymbol{\omega}\,. \tag{3.8}$$

Next, we substitute (2.23a), (2.24a), and (3.3) into (3.2a), and let $\varepsilon \to 0$, to obtain the eigenvalue problem

$$\phi_j'' - \phi_j + 2u_c\phi_j + \frac{1}{v_j^2}\eta_j u_c^2 = \lambda\phi_j\,, \qquad -\infty < y < \infty\,, \tag{3.9}$$

for $j = 1, .., k$. Here $\eta_j = \eta(x_j)$ and $\phi_j(y) \to 0$ as $y \to \infty$. Using (3.7) and (3.8), we can write (3.9) in vector form as

$$\boldsymbol{\phi}'' - \boldsymbol{\phi} + 2u_c\boldsymbol{\phi} - 2u_c^2\left(\frac{\int_{-\infty}^{\infty} u_c\,\mathcal{E}\boldsymbol{\phi}\,dy}{\int_{-\infty}^{\infty} u_c^2\,dy}\right) = \lambda\boldsymbol{\phi}\,. \tag{3.10}$$

Here the symmetric matrix $\mathcal{E}$ is defined by

$$\mathcal{E} = \mathcal{C}\,(\mathcal{B} + \mathcal{C})^{-1}\,. \tag{3.11}$$

We decompose $\mathcal{E}$ as

$$\mathcal{E} = \mathcal{S}^{-1}\Lambda_e\mathcal{S}\,, \tag{3.12}$$

for some nonsingular matrix $\mathcal{S}$ and diagonal matrix Λ_e, which contains the eigenvalues of $\mathcal{E}$. Then, upon defining $\boldsymbol{\psi} = \mathcal{S}\boldsymbol{\phi}$, we obtain from (3.10) that

$$\boldsymbol{\psi}'' - \boldsymbol{\psi} + 2u_c\boldsymbol{\psi} - 2u_c^2\left(\frac{\int_{-\infty}^{\infty} u_c\Lambda_e\boldsymbol{\psi}\,dy}{\int_{-\infty}^{\infty} u_c^2\,dy}\right) = \lambda\boldsymbol{\psi}\,, \qquad -\infty < y < \infty\,, \tag{3.13a}$$

$$\boldsymbol{\psi} \to 0\,, \quad \text{as} \quad |y| \to \infty\,. \tag{3.13b}$$

Since Λ_e is a diagonal matrix we get k uncoupled scalar problems from (3.13).

The final step in the stability analysis is to determine the conditions for which $\mathrm{Re}(\lambda) < 0$ in (3.13). For this we need the following key result of Wei (cf. [17]) in the form written in Appendix E of [6].

Theorem(**Wei [17] and [6]**): *Let $\zeta > 0$ and consider the nonlocal eigenvalue problem for $\phi(y)$*

$$\phi'' - \phi + 2u_c\phi - \zeta u_c^2 \left(\frac{\int_{-\infty}^{\infty} u_c \phi \, dy}{\int_{-\infty}^{\infty} u_c^2 dy} \right) = \lambda \phi \,, \qquad -\infty < y < \infty \,, \tag{3.14a}$$

$$\phi \to 0 \quad \text{as} \quad |y| \to \infty \,, \tag{3.14b}$$

corresponding to eigenpairs for which $\lambda \neq 0$. Here $u_c(y)$ is given in (2.4). The following result pertains to the eigenvalue $\lambda_0 \neq 0$ of (3.14) with the largest real part:

- *If $\zeta < 1$ then $Re(\lambda_0) > 0$,*
- *If $\zeta > 1$ then $Re(\lambda_0) < 0$.*

Comparing (3.13) and (3.14) we conclude that an asymmetric equilibrium spike pattern will be stable with respect to the large $O(1)$ eigenvalues when the minimum eigenvalue e_1 of the matrix $\mathcal{E}$ in (3.11) exceeds the threshold $e_1 > 1/2$. However, it is preferable to express our key stability result in terms of the matrix $\mathcal{E}^{-1}$, which is the product of two tridiagonal matrices. Our main stability result is summarized as follows:

Proposition 3.1 (Asymmetric Patterns): *Let $\lambda_0 \neq 0$ be the eigenvalue of (3.13) with the largest real part. Let e_m be the maximum eigenvalue of the matrix $\mathcal{E}^{-1} = \mathcal{B}\mathcal{C}^{-1} + I$, where I is the identity matrix, Then, $Re(\lambda_0) < 0$ when*

$$e_m < 2 \,, \tag{3.15}$$

and $Re(\lambda_0) > 0$ when $e_m > 2$.

In the special case where the spike pattern is symmetric, as studied in [7], it follows that $v_j = 6bk$ for $j = 1, .., k$, and $d_j = 2/k$ for $j = 2, .., k$. Thus, in this symmetric case, the matrices $\mathcal{C}$ and $\mathcal{B}$ in (3.7) become

$$\mathcal{C} = \frac{1}{6bDk^2} I \,, \qquad \mathcal{B} = \frac{k}{2} \mathcal{B}_0 \,, \quad \text{where} \quad \mathcal{B}_0 \equiv \begin{pmatrix} 1 & -1 & 0 & \cdots & 0 & 0 & 0 \\ -1 & 2 & \ddots & \ddots & \ddots & 0 & 0 \\ 0 & \ddots & \ddots & \ddots & \ddots & \ddots & 0 \\ \vdots & \ddots & \ddots & \ddots & \ddots & \ddots & \vdots \\ 0 & \ddots & \ddots & \ddots & \ddots & \ddots & 0 \\ 0 & 0 & \ddots & \ddots & \ddots & 2 & -1 \\ 0 & 0 & 0 & \cdots & 0 & -1 & 1 \end{pmatrix} . \tag{3.16}$$

Thus, the matrix $\mathcal{E}^{-1}$ in Proposition 3.1 is

$$\mathcal{E}^{-1} = 3bDk^3\mathcal{B}_0 + I\,. \tag{3.17}$$

The eigenvalues μ_j of $\mathcal{B}_0$ are readily calculated as

$$\mu_j = 2\left[1 - \cos\left(\frac{\pi(j-1)}{k}\right)\right], \qquad \text{for} \quad j = 1, .., k\,. \tag{3.18}$$

The maximum eigenvalue of $\mathcal{B}_0$ is μ_k. Thus, the maximum eigenvalue e_m of $\mathcal{E}^{-1}$ is $e_m = 3bDk^3\mu_k + 1$. Using this value in (3.15) of Proposition 3.1 we recover the following stability result of [7] for symmetric patterns.

Corollary 3.1 (Symmetric Patterns): *Let $\lambda_0 \neq 0$ be the eigenvalue of (3.13) with the largest real part. Then, for $\varepsilon \to 0$ and $k \geq 2$, $Re(\lambda_0) < 0$ when*

$$D < D_k \equiv \left(6bk^3\left[1 + \cos\left(\pi/k\right)\right]\right)^{-1}, \tag{3.19}$$

and $Re(\lambda_0) > 0$ when $D > D_k$. When $k = 1$, then $D_1 = \infty$.

4 Examples of the Theory

We now give some analytical and numerical predictions obtained from our existence and stability criteria for asymmetric patterns with four or fewer spikes. The existence criterion for asymmetric equilibria does not depend on the specific orientation of the spikes on the interval. However, for solutions with three or more spikes, the stability criterion with respect to the $O(1)$ eigenvalues does depend on the specific ordering of the spikes on the interval.

4.1 Two-Spike Patterns

For the case of two spikes where $k_1 = k_2 = 1$ we can show that the two-spike pattern exists and is stable when $D_e < D < D_m$. The pattern loses its stability with respect to the large eigenvalues when $D < D_e$.

To obtain an explicit value for D_e, we calculate the matrix $\mathcal{E}^{-1} = \mathcal{B}\mathcal{C}^{-1} + I$ in Proposition 3.1 analytically. Using (3.7b) for $\mathcal{B}$ and (3.7a) for $\mathcal{C}$, we get

$$\mathcal{E}^{-1} = I + \frac{6bD}{d_2}\begin{pmatrix} l_1^{-2} & -l_2^{-2} \\ -l_1^{-2} & l_2^{-2} \end{pmatrix}, \tag{4.1}$$

where I is the 2×2 identity matrix. Since $d_2 = l_1 + l_2 = 1$ and $l_j = qz_j$, where q is defined in (2.10a), (4.1) becomes

$$\mathcal{E}^{-1} = I + \frac{6bD}{q^2} \begin{pmatrix} z_1^{-2} & -z_2^{-2} \\ -z_1^{-2} & z_2^{-2} \end{pmatrix} . \tag{4.2}$$

The maximum eigenvalue e_m of $\mathcal{E}^{-1}$ in (4.2) is readily calculated as

$$e_m = \frac{6bD}{q^2} \left(z_1^{-2} + z_2^{-2} \right) + 1 . \tag{4.3}$$

Substituting (4.3) into the stability criterion (3.15), we obtain that the pattern is stable if and only if

$$\frac{1}{z_1^2} + \frac{1}{z_2^2} < \frac{4}{q} . \tag{4.4}$$

Setting $k_1 = k_2 = 1$ in (2.14), we conclude that $z_1^2 + 1/z_1 = z_2^2 + 1/z_2$ and $z_1 + z_2 = 1/q$. Thus, $z_1 z_2 = q$. Substituting these formulae into (4.4), and solving for q, we obtain that the two-spike pattern is stable when $q^3 > 1/6$, where $q = (24bD)^{1/3}$ from (2.10a). This leads to the following key result:

Result 4.1(Two Spikes): *Let $k_1 = k_2 = 1$ and $\varepsilon \to 0$. Then, a two-spike pattern of the form AB or BA exists and is stable with respect to the large $O(1)$ eigenvalues when D satisfies*

$$\frac{b^{-1}}{144} < D < \frac{b^{-1}}{96} \tag{4.5}$$

The upper bound in (4.5) is the existence bound given in (2.16a). The pattern loses its stability when D is decreased below the lower bound in (4.5). Notice that the stability criterion here is the same for both AB and AB patterns.

In Fig. 4 we plot u from Proposition 2.1 for AB patterns at three different values of D. In this figure, the plots with $D = 0.010$ and $D = 0.008$ represent stable equilibria. The solution with $D = 0.006$ is an unstable equilibrium solution.

4.2 Three-Spike Patterns

Similar results can be obtained for a three-spike pattern. Using (3.7) for $\mathcal{B}$ and $\mathcal{C}$, we get that $\mathcal{E}^{-1} = \mathcal{B}\mathcal{C}^{-1} + I$ satisfies

$$\mathcal{E}^{-1} = 6bD\hat{\mathcal{E}} + I , \quad \text{where} \quad \hat{\mathcal{E}} \equiv \begin{pmatrix} e_{11} & e_{12} & 0 \\ e_{21} & e_{22} & e_{23} \\ 0 & e_{32} & e_{33} \end{pmatrix} , \tag{4.6a}$$

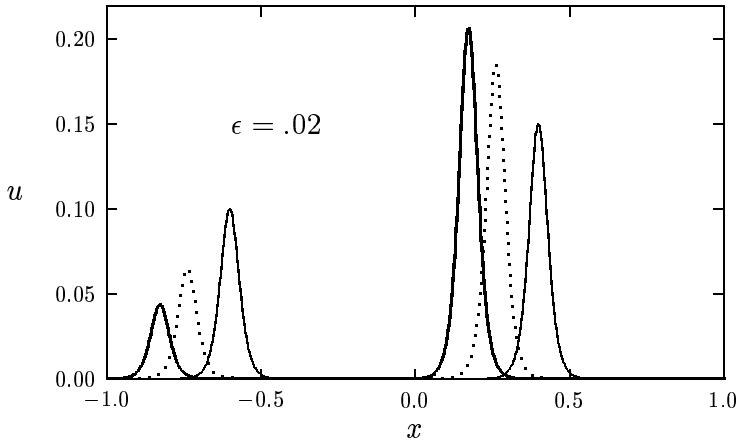

Figure 4: Plots of u versus x for a two-spike asymptotic asymmetric equilibrium solution of the form AB with $D = .010$ (solid curve), $D = 0.008$ (dotted curve), and $D = 0.006$ (heavy solid curve). Also, $\epsilon = .02$ and $b = 1$.

where the entries e_{ij} are defined by

$$\begin{gathered} e_{11} = l_1^{-2}(l_1+l_2)^{-1}\,, \quad e_{12} = -l_2^{-2}(l_1+l_2)^{-1}\,, \quad e_{21} = -l_1^{-2}(l_1+l_2)\,, \\ e_{22} = l_2^{-2}\left[(l_1+l_2)^{-1} + (l_2+l_3)^{-1}\right]\,, \qquad e_{23} = -l_3^{-2}(l_2+l_3)^{-1}\,, \\ e_{32} = -l_2^{-2}(l_2+l_3)^{-1}\,, \qquad e_{33} = l_3^{-2}(l_2+l_3)\,. \end{gathered} \tag{4.6b}$$

Let σ be an eigenvalue of $\hat{\mathcal{E}}$. As shown in Result 4.7 of §4.3 below, $\hat{\mathcal{E}}$ has an eigenvalue of zero. The other two eigenvalues of $\hat{\mathcal{E}}$ are found to satisfy

$$\sigma^2 - \sigma\kappa_t + \kappa_d = 0\,. \tag{4.7a}$$

Here κ_d and κ_t, which is the trace of $\hat{\mathcal{E}}$, are defined in terms of the e_{ij} by

$$\kappa_t = e_{11} + e_{22} + e_{33}\,, \qquad \kappa_d = e_{11}e_{22} + e_{11}e_{33} + e_{22}e_{33} - e_{23}e_{32} - e_{21}e_{12}\,. \tag{4.7b}$$

Thus, we can calculate the maximum eigenvalue e_m of $\mathcal{E}^{-1}$ needed in Proposition 3.1. In this way, we obtain the following stability result:

Result 4.2(Three Spikes): *Let $k = 3$ and $\varepsilon \to 0$. Assume that D is such that a three-spike pattern exists, where z and $\tilde{z}$ are computed from (2.14). Then, the pattern is stable with respect to the large $O(1)$ eigenvalues when*

$$\left(\kappa_t + \sqrt{\kappa_t^2 - 4\kappa_d}\right) < \frac{1}{3bD}\,, \tag{4.8}$$

and it is unstable when the inequality in (4.8) is reversed.

Let D_e be the critical value of D where the stability changes. Then, D_e is the value of D for which

$$\kappa_t + \sqrt{\kappa_t^2 - 4\kappa_d} = \frac{1}{3bD}\,. \tag{4.9}$$

Equations (4.9) and (2.14) form a coupled system for z, $\tilde{z}$ and D_e. This system, which is solved by Newton's method, depends on k_1, k_2, and on the specific ordering of the small and large spikes on the interval. However, by examining (4.9), with the e_{ij} as defined in (4.6b), it is clear that AAB and BAA patterns have the same stability criterion as do those of the form BBA and ABB.

We first consider the case $k_1 = 1$ and $k_2 = 2$ so that no solution multiplicity occurs. There are two different values of D_e depending on the two orientations ABB and BAB. We obtain the following numerical results:

Result 4.3(Three Spikes): *Let $k_1 = 1$, $k_2 = 2$, and $\varepsilon \to 0$. Then, a three-spike pattern exists and is stable with respect to the large $O(1)$ eigenvalues when D satisfies*

$$ABB \quad \text{pattern}\,; \quad \to \quad 0.00122/b < D < 0.00308/b\,, \tag{4.10a}$$

$$BAB \quad \text{pattern}\,; \quad \to \quad 0.00224/b < D < 0.00308/b\,. \tag{4.10b}$$

The three-spike pattern loses its stability when D is decreased below the lower bounds in (4.10). The upper bounds are the values of D_m given in Result 2.4.

In Fig. 5(a) and Fig. 5(b) we plot u versus x for BAB and ABB patterns, respectively. For each pattern we plot the solution at two different values of D. All of these solutions are stable with respect to the $O(1)$ eigenvalues except for the BAB pattern in Fig. 5(a) with $D = .002$.

Now we consider the case where $k_1 = 2$ and $k_2 = 1$. In this case, solution multiplicity occurs for the range of D given in Result 2.5. There are two patterns to consider: AAB and ABA. As an example, in Fig. 6 we plot the two solutions of the form ABA that exist when $D = 0.0035$ and $b = 1$. The solid curve in this figure, corresponding to the larger value of z, is stable. The dotted curve, corresponding to the smaller value of z, is unstable.

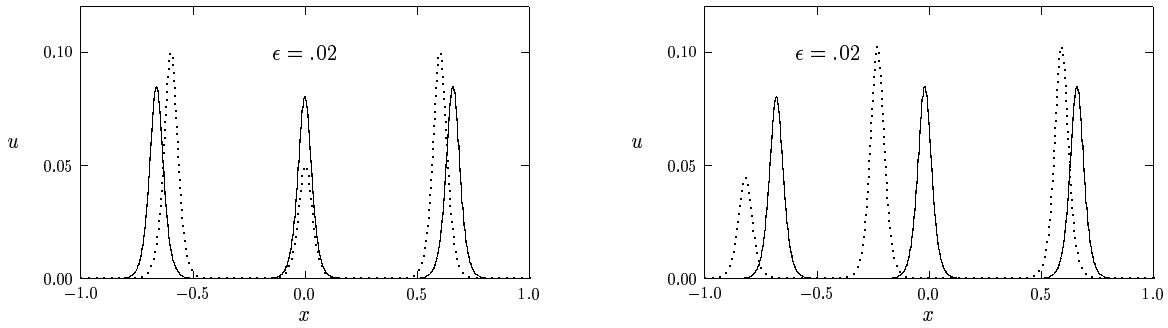

(a) BAB pattern: $D = 0.003$ (solid curve), $D = 0.002$ (dotted curve)

(b) ABB pattern: $D = 0.003$ (solid curve), $D = 0.0018$ (dotted curve)

Figure 5: Plots of u versus x for a three-spike asymptotic asymmetric equilibrium solution of the form BAB and ABB for two different values of D with $\epsilon = .02$ and $b = 1$.

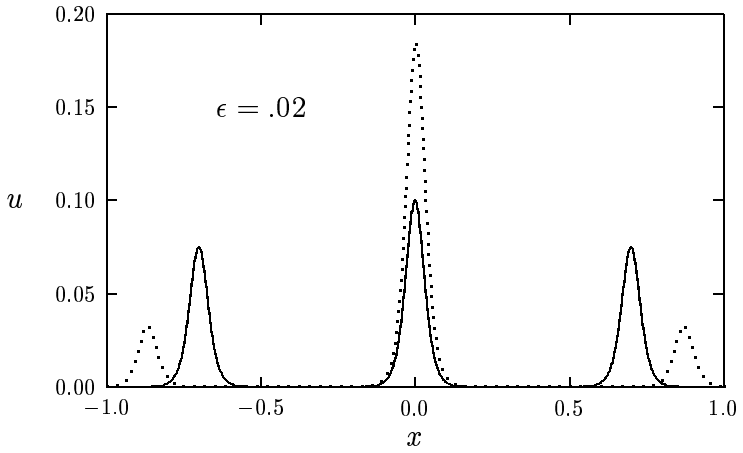

Figure 6: Plots of u versus x exhibiting solution multiplicity for a three-spike pattern of the form ABA. The parameter values are $D = 0.0035$, $\epsilon = .02$, and $b = 1$. The solid curve, corresponding to the larger root, is stable. The dotted curve, corresponding to the smaller root, is unstable.

To find the critical value D_e of D, where the stability of each of these patterns is exchanged, we must solve the coupled system (2.14) and (4.9) numerically. In this way, we obtain the numerical values

$$D_e = .00347/b \qquad \text{AAB pattern}\,; \qquad D_e = .00396/b \qquad \text{ABA pattern}\,. \tag{4.11}$$

For the AAB pattern this exchange of stability occurs for the larger root of (2.14). In contrast, the exchange of stability for the ABA pattern occurs for the smaller root to (2.14).

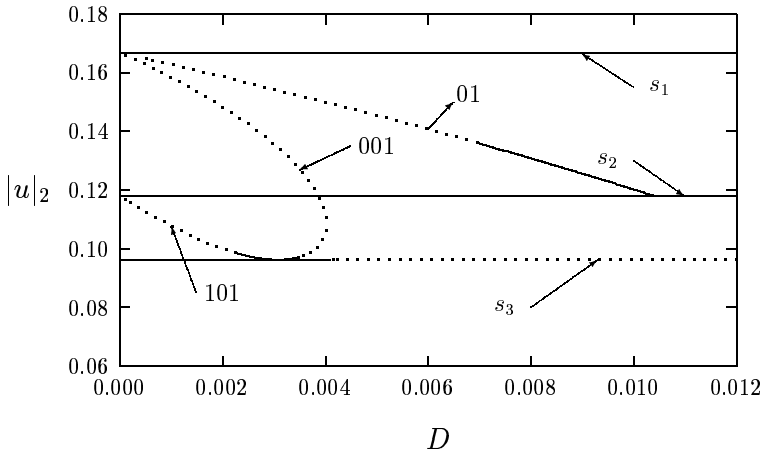

Figure 7: Plot of $|u|_2$ defined in (4.12) versus D for solutions with three or fewer spikes with $b = 1$. The symmetric branch with k spikes is s_k. The asymmetric patterns AB, BAB, and AAB are labeled by 01, 101, and 001, respectively. The portions of the branches that are solid (dotted) are stable (unstable) with respect to the large $O(1)$ eigenvalues.

Finally, in Fig. 7 we take $b = 1$ and we plot a bifurcation diagram showing the relationship between the symmetric and asymmetric solution branches. The vertical axis in this figure is the $|u|_2$ norm defined by

$$|u|_2 \equiv \left(\sum_{j=1}^{k} v_j^{-2} \right)^{1/2} . \tag{4.12}$$

In this figure, we label by s_k the symmetric branch for which k spikes have equal height. In the symmetric case, $v_j = 6bk$ for $j = 1, .., k$, so that $|u|_2 = 1/(6b\sqrt{k})$. From (3.19) the branch s_k is

stable with respect to the large $O(1)$ eigenvalues when $D < D_k$. In Fig. 7, the portions of the solution branches that are stable with respect to the large $O(1)$ eigenvalues are given by the solid lines. Portions of these branches that are unstable are dotted. In plotting the asymmetric solution branches, we note that a pattern such as ABA traces out exactly the same curve in this figure as an AAB pattern, except that their stability properties are different. In each case when plotting a connecting asymmetric branch, we have plotted the one that is maximally unstable (i. e. the one that goes unstable for the largest value of D).

4.3 Four-Spike Patterns

When there are four spikes we determine the maximum eigenvalue e_m of Proposition 3.1 numerically using LAPACK [1]. Setting $e_m = 2$ gives the critical stability value D_e. Patterns that have the values of D_e are AABB and BBAA, BABA and ABAB, AAAB and BAAA, ABBB and BBBA. When $k_1 \leq k_2$ we obtain the following results:

Result 4.4(Four Spikes): *Let $k_1 \leq k_2$ and $\varepsilon \to 0$. Then, a four-spike pattern exists and is stable with respect to the large $O(1)$ eigenvalues when D satisfies*

$$ABBB \quad \text{pattern}; \quad \to \quad 0.00041/b < D < 0.00130/b\,, \tag{4.13a}$$

$$BABB \quad \text{pattern}; \quad \to \quad 0.00085/b < D < 0.00130/b\,, \tag{4.13b}$$

$$AABB \quad \text{pattern}; \quad \to \quad 0.00128/b < D < 0.00130/b\,, \tag{4.13c}$$

$$BABA \quad \text{pattern}; \quad \to \quad 0.00122/b < D < 0.00130/b\,. \tag{4.13d}$$

These values suggest that solutions with fewer small spikes have wider stability regions than those with more small spikes.

In Fig. 8(a) and Fig. 8(b) we set $b = 1$ and plot u versus x for the patterns BABA and BABB, respectively. In each figure we plot the solution for two values of D. The solutions in these figures corresponding to the larger (smaller) value of D is stable (unstable) with respect to the $O(1)$ eigenvalues.

Solution multiplicity is possible when $k_1 = 3$ and $k_2 = 1$. As an example, in Fig. 9 we plot the two solutions for an AABA pattern that exist when $D = 0.0023$, $k_1 = 3$, $k_2 = 1$ and $b = 1$. Both of these solutions are unstable. The only two patterns with different stability criteria are AAAB and AABA. To find the critical value D_e where the stability of each of these patterns is exchanged, we solve the coupled system (2.14) and (4.9) numerically. In this way, we obtain the numerical values

$$D_e = 0.00142/b \qquad \text{AAAB pattern}; \qquad D_e = 0.00154/b \qquad \text{AABA pattern}\,. \tag{4.14}$$

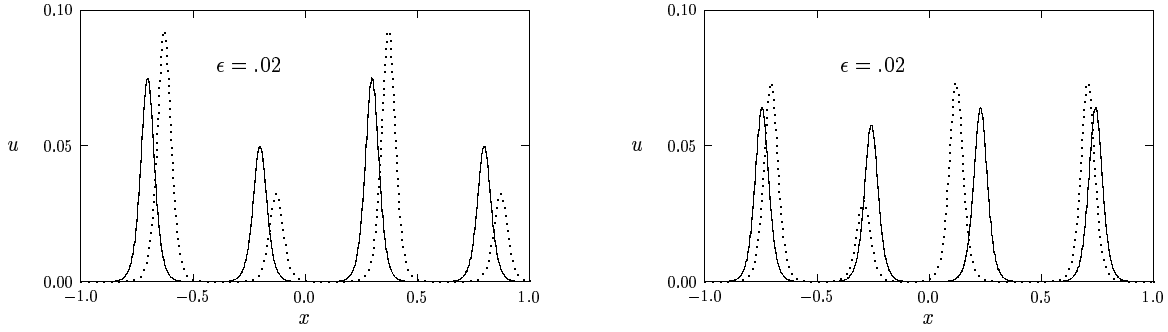

(a) BABA pattern: $D = .00125$ (solid curve), $D = 0.001$ (dotted curve)

(b) BABB pattern: $D = .0012$ (solid curve), $D = 0.0006$ (dotted curve)

Figure 8: Plot of u versus x for a four-spike asymptotic asymmetric equilibrium solution of the form BABA and BABB for two different values of D with $\epsilon = .02$ and $b = 1$.

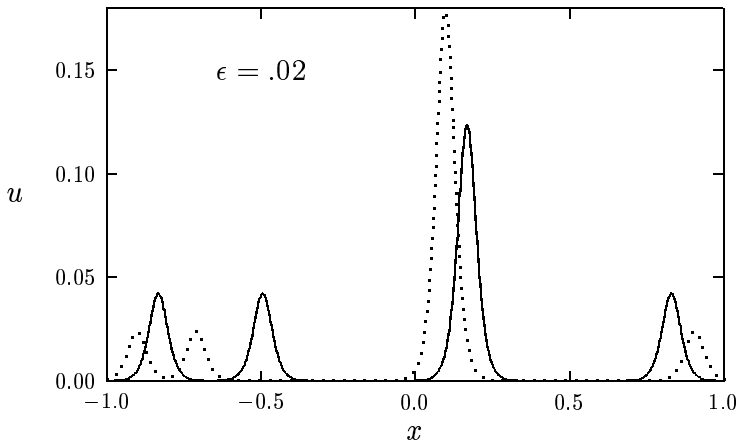

Figure 9: Plot of u versus x for a four-spike asymptotic asymmetric equilibrium solution of the form AABA in the region where solution multiplicity occurs. The parameters are $D = 0.0023$, $\epsilon = .02$, and $b = 1$. The solid curve corresponds to the larger root of (2.14) while the dotted curve corresponds to the smaller root.

For both patterns this exchange of stability occurs for the larger root of (2.14).

Similar to Fig. 7, a plot (not shown) of the $|u|_2$ norm versus D shows that an asymmetric solution with $m > 0$ small spikes provides the transition between the symmetric branches s_k and s_{k-m}.

4.4 A Few General Results

For $k \leq 3$, we have shown numerically that an asymmetric branch with $i > 0$ small spikes provides the connection between the symmetric branches s_k and s_{k-i}. This connection property should holds for higher values of k. We now show that for any k, with $k \geq 2$, the asymmetric branches that emerge from the symmetric branch s_k when $D = D_m$ are stable with respect to the $O(1)$ eigenvalues at least sufficiently close to the bifurcation point. This result is summarized as follows.
Result 4.5: *An asymmetric branch that emerges from the symmetric branch s_k is always stable with respect to the large $O(1)$ eigenvalues for $D - D_m$ sufficiently small.*

To show this result, we first note that the symmetric branch s_k is stable when $D < D_k$, where D_k is given in (3.19). The asymmetric branch bifurcates from s_k when $D = D_m$, where D_m is given in (2.16a). By comparing (3.19) and (2.16a) it is clear than $D_m < D_k$. By continuity of matrix eigenvalues with respect to small perturbations of a nonsingular matrix, the stability criterion (3.15) for the asymmetric branches must hold sufficiently close to D_m. Hence the result 4.5 follows.

The next result shows a scaling property, with respect to the parameter b, for the range of values of D where asymmetric equilibria exist and are stable with respect to the $O(1)$ eigenvalues.
Result 4.6: *Let k_1 and k_2 be non-negative integers and $\varepsilon \to 0$. Then, we can find constants $D^*_{m_1}$ and D^*_e, independent of the parameter b, such that an asymmetric pattern exists and is stable with respect to the $O(1)$ eigenvalues on the interval $D^*_e b^{-1} < D < D^*_{m_1} b^{-1}$.*

This result follows readily from the definition of the matrix $\mathcal{E}^{-1}$ in Proposition 3.1. The matrix $\mathcal{B}$ in (3.7b) depends only on the product bD. In addition, since $v_j = 6b/l_j$, it is clear from (3.7a) that the matrix $\mathcal{C}^{-1}$ also only depends on the product bD. Hence, $\mathcal{E}^{-1}$ depends only on the product bD and the scaling result given above holds.

The final result concerns an eigenvalue of the stability matrix $\mathcal{E}^{-1}$ defined in Proposition 3.1.
Result 4.7: *The matrix $\mathcal{E}^{-1} = \mathcal{B}\mathcal{C}^{-1} + I$ always has the value one as an eigenvalue.*

From the definition of $\mathcal{B}$ in (3.7b), we observe that $\mathcal{B}\boldsymbol{\zeta} = \mathbf{0}$, where $\boldsymbol{\zeta}^t = (1, .., 1)$ and $\mathbf{0}$ is the zero vector. Thus, $\mathcal{E}^{-1}\boldsymbol{\eta} = \boldsymbol{\eta}$, where $\boldsymbol{\eta} = \mathcal{C}\boldsymbol{\zeta}$, and the result follows.

5 The Stability Analysis: Small Eigenvalues

In this section we analyze the small eigenvalues of order $O(\varepsilon^2)$ in the spectrum of (3.2). These eigenvalues may generate instabilities on a long time scale $t = O(\varepsilon^{-2})$. We determine the range of D for which these eigenvalues are in the stable left half-plane. In §5.1 we reduce (3.2) to the study of a matrix eigenvalue problem. In §5.2 we analyze this matrix eigenvalue problem and compute the eigenvalues numerically.

5.1 Deriving the Matrix Eigenvalue Problem

We first write (3.2) in the form

$$L_\varepsilon \phi + u_e^2 \eta = \lambda \phi \,, \qquad -1 < x < 1 \,, \tag{5.1a}$$

$$D\eta_{xx} - \frac{b}{\varepsilon} u_e^2 \eta = \frac{2b}{\varepsilon} v_e u_e \phi \,, \qquad -1 < x < 1 \,, \tag{5.1b}$$

$$\phi_x(\pm 1) = \eta_x(\pm 1) = 0 \,. \tag{5.1c}$$

Here

$$L_\varepsilon \phi \equiv \varepsilon^2 \phi_{xx} - \phi + 2 v_e u_e \phi \,, \tag{5.1d}$$

while u_e and v_e are given by

$$u_e \sim \sum_{j=1}^{k} v_j^{-1} u_j \,; \qquad v_e \sim \sum_{j=1}^{k} \frac{6b}{v_j} G(x; x_j) + \bar{v} \,. \tag{5.2}$$

We have defined $u_j(y) \equiv u_c\left[\varepsilon^{-1}(x - x_j)\right]$, where $u_c(y)$ is given in (2.4). Also, v_j, $\bar{v}$ and x_j are given in (2.23b), (2.26), and (2.27), respectively. The brackets are defined by $\langle \zeta \rangle_j \equiv (\zeta(x_{j+}) + \zeta(x_{j-}))/2$ and $[\zeta]_j \equiv \zeta(x_{j+}) - \zeta(x_{j-})$, where $\zeta(x_{j\pm})$ are the one-sided limits of $\zeta(x)$ as $x \to x_{j\pm}$. The spike locations x_j are such that

$$\langle v_{ex} \rangle_j = 0 \,, \qquad j = 1, .., k \,. \tag{5.3}$$

Next, we differentiate the equilibrium problem for (1.6a) with respect to x to get

$$L_\varepsilon u_{ex} = -u_\varepsilon^2 v_{\varepsilon x} \,. \tag{5.4}$$

Thus, for x near x_j, we get

$$L_\varepsilon u_j' \sim -\varepsilon v_j^{-1} u_j^2 v_{ex} \,. \tag{5.5}$$

This suggests that we expand

$$\phi = \phi_0 + \varepsilon\phi_1 + \cdots , \qquad \eta(x) = \varepsilon\eta_0(x) + \cdots , \tag{5.6a}$$

where

$$\phi_0 \equiv \sum_{j=1}^{k} c_j u_j^{'} \left[\varepsilon^{-1}(x - x_j)\right] , \qquad \phi_1 \equiv \sum_{j=1}^{k} c_j \phi_{1j} \left[\varepsilon^{-1}(x - x_j)\right] . \tag{5.6b}$$

Here the c_j are arbitrary coefficients.

We substitute (5.6a) into (5.1a) and use (5.5) and $\lambda = O(\varepsilon^2)$. For x near x_j, we get that $\phi_{1j}(y)$ satisfies

$$c_j L_\varepsilon \phi_{1j} \sim \frac{u_j^2}{v_j} \left[c_j v_{ex}(x_j + \varepsilon y) - \frac{\eta_0(x_j + \varepsilon y)}{v_j} \right] . \tag{5.7}$$

Before solving this equation for ϕ_{1j} we need to determine an important continuity property of the right-hand side of (5.7).

Substituting (5.6a) into (5.1b), we get that η_0 satisfies

$$D\eta_{0xx} - \frac{b}{\varepsilon} u_e^2 \eta_0 = \frac{2b}{\varepsilon^2} v_e u_e \left(\phi_0 + \varepsilon\phi_1\right) , \qquad -1 < x < 1 . \tag{5.8}$$

Since ϕ_0 is a linear combination of $u_j^{'}$, it follows that the term multiplied by ϕ_0 on the right-hand side in (5.8) behaves like a dipole. Hence, for $\varepsilon \ll 1$, this term is a linear combination of $\delta^{'}(x - x_j)$ for $j = 1, .., k$, where $\delta(x)$ is the delta function. Thus, η_0 will be discontinuous across $x = x_j$. However, if we define the function $f(x)$ by

$$f(x) \equiv c_j v_{ex}(x) - \frac{\eta_0(x)}{v_j} , \tag{5.9}$$

then f is continuous across $x = x_j$. To see this, we differentiate (1.6b) for v_e with respect to x and subtract appropriate multiples of the resulting equation and (5.8) to find that the dipole term cancels exactly. Thus, f is continuous across $x = x_j$, and we have $\langle f \rangle_j = f(x_j)$. However, $\langle v_{ex} \rangle_j = 0$ from (5.3). Hence, $f(x_j) = -v_j^{-1} \langle \eta_0 \rangle_j$. Therefore, for $\varepsilon \ll 1$, we get from (5.7) that ϕ_{1j} satisfies

$$c_j L_\varepsilon \phi_{1j} \sim -\frac{u_j^2}{v_j^2} \langle \eta_0 \rangle_j . \tag{5.10}$$

Since $L_\varepsilon u_j = u_j^2 + O(\varepsilon)$, we can solve (5.10) as

$$c_j \phi_{1j}(y) = -\frac{1}{v_j^2} u_j(y) \langle \eta_0 \rangle_j + O(\varepsilon)\,. \tag{5.11}$$

Equation (5.11) shows that ϕ_{1j} is continuous across $x = x_j$ and has the form of a spike. This implies that the term in (5.8) proportional to ϕ_1 behaves like a linear combination of $\delta(x-x_j)$ when $\varepsilon \ll 1$ and, most importantly, has *the same asymptotic order* in ε as the dipole term proportional to ϕ_0. This shows the fact that we need to determine the approximate eigenfunction for ϕ to both the $O(1)$ and $O(\varepsilon)$ terms in order to calculate an eigenvalue of order $O(\varepsilon^2)$.

Next, let $\varepsilon \to 0$ and use (5.6b) to calculate for x near x_j that

$$\frac{2b}{\varepsilon^2} v_e u_e c_j u_j^{'} \sim 6 b c_j\, \delta^{'}(x - x_j)\,, \tag{5.12a}$$

$$\frac{b}{\varepsilon} u_e^2 \sim \frac{6b}{v_j^2}\, \delta(x - x_j)\,. \tag{5.12b}$$

Substituting (5.12) into (5.8), and using the formula (5.11) for ϕ_{1j}, we get

$$D\eta_{0xx} - 6b \left[\sum_{j=1}^{k} v_j^{-2} \delta(x - x_j) \right] \eta_0 = 6b \sum_{j=1}^{k} c_j \delta^{'}(x - x_j) - \sum_{j=1}^{k} \frac{12b}{v_j^2} \langle \eta_0 \rangle_j \delta(x - x_j)\,. \tag{5.13}$$

This problem is equivalent to

$$D\eta_{0xx} = 0\,, \qquad -1 < x < 1\,; \qquad \eta_{0x}(\pm 1) = 0\,, \tag{5.14a}$$

$$[D\eta_0]_j = 6bc_j\,; \qquad [D\eta_{0x}]_j = -\frac{6b}{v_j^2} \langle \eta_0 \rangle_j\,. \tag{5.14b}$$

To estimate the small eigenvalue we substitute (5.6) into (5.1a) and multiply both sides of (5.1a) by $u_j^{'}$. Upon integrating the resulting equation across the domain we get

$$\sum_{i=1}^{k} \left(u_j^{'}, c_i L_\varepsilon u_i^{'} \right) + \varepsilon \sum_{i=1}^{k} \left(u_j^{'}, c_i L_\varepsilon \phi_{1i} \right) + \varepsilon \left(u_j^{'}, u_e^2 \eta_0 \right) \sim \lambda \sum_{i=1}^{k} \left(c_i u_i^{'}, u_j^{'} \right)\,. \tag{5.15}$$

Here $(f, g) \equiv \int_{-1}^{1} f(x) g(x)\, dx$. To within negligible exponentially small terms, the dominant contribution in the sum comes from $i = j$ since $u_j^{'}$ is exponentially localized near $x = x_j$. Thus, (5.15) becomes

$$c_j \left(u_j^{'}, L_\varepsilon u_j^{'} \right) + \varepsilon c_j \left(u_j^{'}, L_\varepsilon \phi_{1j} \right) + \frac{\varepsilon}{v_j^2} \left(u_j^{'}, u_j^2 \eta_0 \right) \sim \lambda c_j \left(u_j^{'}, u_j^{'} \right)\,. \tag{5.16}$$

Since L_ε is self-adjoint, we integrate by parts on the second term on the left-hand side of (5.16) and use (5.5) for $L_\varepsilon u_j^{'}$. Since the integrands in (5.16) are localized near $x = x_j$, we can write the resulting integrals in terms of the stretched variable $y = \varepsilon^{-1}(x - x_j)$ to get

$$-\varepsilon^2 \int_{-\infty}^{\infty} \frac{u_j^2 u_j^{'}}{v_j} \left[v_{ex} c_j - \frac{\eta_0}{v_j} \right] dy - \varepsilon^3 c_j \int_{-\infty}^{\infty} \frac{u_j^2}{v_j} v_{ex} \phi_{1j}\, dy \sim \varepsilon \lambda c_j \int_{-\infty}^{\infty} \left(u_c^{'} \right)^2 dy\,. \tag{5.17}$$

In this expression $\eta_0 = \eta_0(x_j + \varepsilon y)$ and $v_{ex} = v_{ex}(x_j + \varepsilon y)$.

We now estimate each of the terms in (5.17). Since $[\phi_{1j}]_j = 0$, $\langle v_{ex} \rangle_j = 0$, and $u_j^{'}$ is odd, it follows that the second integral on the left-hand side of (5.17) will be $o(\varepsilon^3)$ and can be neglected. Thus, from (5.17) we obtain

$$\varepsilon \lambda c_j \int_{-\infty}^{\infty} \left(u_c^{'} \right)^2 dy \sim -\varepsilon^2 \int_{-\infty}^{\infty} \frac{u_j^2 u_j^{'}}{v_j} f(x_j + \varepsilon y)\, dy\,, \tag{5.18}$$

where $f(x)$ is defined in (5.9). The function f is continuous across $x = x_j$ but its derivative is not. For $\varepsilon \ll 1$, we integrate by parts in (5.18) to obtain

$$\varepsilon \lambda c_j \int_{-\infty}^{\infty} \left(u_c^{'} \right)^2 dy \sim \frac{\varepsilon^3}{3 v_j} \int_{-\infty}^{\infty} u_c^3\, dy\ \langle f^{'} \rangle_j\,. \tag{5.19}$$

Then, since v_{exx} is continuous across $x = x_j$ and $v_{exx}(x_j) = -1/(2D)$, we obtain

$$\langle f^{'} \rangle_j = c_j v_{exx}(x_j) - \frac{\langle \eta_{0x} \rangle_j}{v_j} = -\frac{c_j}{2D} - \frac{\langle \eta_{0x} \rangle_j}{v_j}\,. \tag{5.20}$$

Finally, substituting (5.20) into (5.19), we obtain the following main result:

Proposition 5.1: *The eigenvalues of order $O(\varepsilon^2)$ for (3.2) satisfy*

$$\lambda c_j \int_{-\infty}^{\infty} \left[u_c^{'}(y) \right]^2 dy \sim -\frac{\varepsilon^2}{3} \int_{-\infty}^{\infty} \left[u_c(y) \right]^3 dy \left(\frac{\langle \eta_{0x} \rangle_j}{v_j^2} + \frac{c_j}{2 D v_j} \right)\,, \qquad j = 1, .., k\,. \tag{5.21}$$

Here $\langle \eta_{0x} \rangle_j$ is to be calculated from (5.14).

5.2 Analyzing the Matrix Eigenvalue Problem

We first define σ in terms of λ by

$$\lambda = \frac{\varepsilon^2}{6D} \left(\frac{\int_{-\infty}^{\infty} \left[u_c(y) \right]^3 dy}{\int_{-\infty}^{\infty} \left[u_c'(y) \right]^2 dy} \right) \sigma\,. \tag{5.22}$$

Then, (5.21) can be written in matrix form as

$$\mathcal{F}\boldsymbol{c} + \sigma\boldsymbol{c} = -\frac{D^2}{3b}\mathcal{C}\langle\boldsymbol{\eta_{0x}}\rangle\,, \tag{5.23}$$

where $\mathcal{C}$ is defined in (3.7a) and

$$\mathcal{F} \equiv \begin{pmatrix} 1/v_1 & 0 & \cdots & 0 \\ 0 & \ddots & \cdots & 0 \\ \vdots & \vdots & \ddots & \vdots \\ 0 & 0 & \cdots & 1/v_k \end{pmatrix}, \qquad \boldsymbol{c} \equiv \begin{pmatrix} c_1 \\ \vdots \\ c_k \end{pmatrix}, \qquad \langle\boldsymbol{\eta_{0x}}\rangle \equiv \begin{pmatrix} \langle\eta_{0x}\rangle_1 \\ \vdots \\ \langle\eta_{0x}\rangle_k \end{pmatrix}. \tag{5.24}$$

Next we must calculate $\langle\boldsymbol{\eta_{0x}}\rangle$ in terms of $\boldsymbol{c}$ from the solution to (5.14). The resulting expression will then be substituted into (5.21).The solution to (5.14) can be written as

$$\eta_0(x) = \sum_{j=1}^{k} \left(6bc_j g(x;x_j) + m_j G(x;x_j)\right) + 2\eta_a\,, \tag{5.25}$$

for some coefficients m_j, for $j = 1,..,k$. Here G satisfies (2.25) and $g(x;x_j)$ is the dipole Green's function satisfying

$$Dg_{xx} = \delta'(x - x_j)\,, \qquad -1 < x < 1\,, \tag{5.26a}$$

$$g_x(\pm 1;x_j) = 0\,, \qquad \int_{-1}^{1} g(x;x_j)\,dx = 0\,. \tag{5.26b}$$

Since G and g have a zero spatial average over the interval $-1 < x < 1$, the unknown constant η_a in (5.25) is the average value of $\eta(x)$ given by $2\eta_a = \int_{-1}^{1}\eta_0\,dx$. The solution to (5.26) is clearly,

$$g(x;x_j) = -\frac{\partial}{\partial_{x_j}} G(x;x_j)\,. \tag{5.27}$$

The jump conditions in (5.14b), together with the requirement that $\sum_{j=1}^{k}\left[D\eta_{0x}\right]_j = 0$, lead us to the following problem for the coefficients m_k:

$$\boldsymbol{m} = -D\mathcal{C}\langle\boldsymbol{\eta_0}\rangle\,, \qquad \boldsymbol{e}^t\boldsymbol{m} = 0\,. \tag{5.28}$$

Here we have defined

$$\boldsymbol{m} \equiv \begin{pmatrix} m_1 \\ \vdots \\ m_k \end{pmatrix}, \qquad \boldsymbol{e} \equiv \begin{pmatrix} 1 \\ \vdots \\ 1 \end{pmatrix}, \qquad \langle\boldsymbol{\eta_0}\rangle \equiv \begin{pmatrix} \langle\eta_0\rangle_1 \\ \vdots \\ \langle\eta_0\rangle_k \end{pmatrix}. \tag{5.29}$$

Using (5.25) we calculate that

$$\langle \boldsymbol{\eta_0} \rangle = 6b\mathcal{P}_g \boldsymbol{c} + \mathcal{G}\boldsymbol{m} + 2\eta_a \boldsymbol{e}\,, \tag{5.30}$$

where $\mathcal{P}_g$ and $\mathcal{G}$ are defined by

$$\mathcal{P}_g \equiv \begin{pmatrix} \langle g(x_1;x_1)\rangle_1 & \cdots & g(x_1;x_k) \\ \vdots & \ddots & \vdots \\ g(x_k;x_1) & \cdots & \langle g(x_k;x_k)\rangle_k \end{pmatrix}, \qquad \mathcal{G} \equiv \begin{pmatrix} G(x_1;x_1) & \cdots & G(x_1;x_k) \\ \vdots & \ddots & \vdots \\ G(x_k;x_1) & \cdots & G(x_k;x_k) \end{pmatrix}. \tag{5.31}$$

Combining (5.28) and (5.30), we determine $\boldsymbol{m}$ as

$$\boldsymbol{m} = -6bD\mathcal{C}\left(I + D\mathcal{G}\mathcal{C}\right)^{-1}\mathcal{P}_g\boldsymbol{c} - 2D\eta_a\mathcal{C}\left(I + D\mathcal{G}\mathcal{C}\right)^{-1}\boldsymbol{e}\,. \tag{5.32}$$

The constraint $\boldsymbol{e}^t\boldsymbol{m} = 0$ determines η_a as

$$\eta_a = -\frac{3b}{\beta}\boldsymbol{e}^t\mathcal{C}\left(I + D\mathcal{G}\mathcal{C}\right)^{-1}\mathcal{P}_g\boldsymbol{c}\,, \qquad \text{where} \qquad \beta \equiv \boldsymbol{e}^t\mathcal{C}\left(I + D\mathcal{G}\mathcal{C}\right)^{-1}\boldsymbol{e}\,. \tag{5.33}$$

Next, by differentiating (5.25), and by noting that $g(x;x_j)$ is piecewise constant, we obtain

$$\langle \boldsymbol{\eta_{0x}} \rangle = \mathcal{P}\boldsymbol{m}\,, \tag{5.34}$$

where

$$\mathcal{P} \equiv \begin{pmatrix} \langle G_x(x_1;x_1)\rangle_1 & \cdots & G_x(x_1;x_k) \\ \vdots & \ddots & \vdots \\ G_x(x_k;x_1) & \cdots & \langle G_x(x_k;x_k)\rangle_k \end{pmatrix}. \tag{5.35}$$

By calculating $\mathcal{P}$ and $\mathcal{P}_g$ explicitly, it is easy to see that

$$\mathcal{P}_g = -\mathcal{P}^t\,. \tag{5.36}$$

Finally, by substituting (5.32) for $\boldsymbol{m}$ into (5.34) we determine $\langle \boldsymbol{\eta_{0x}} \rangle$ in terms of $\boldsymbol{c}$. Substituting this expression for $\langle \boldsymbol{\eta_{0x}} \rangle$ into (5.23) we obtain the following main result:

Proposition 5.2: *For $\varepsilon \ll 1$, the eigenvalues of (3.2) of order $\lambda = O(\varepsilon^2)$ satisfy*

$$\lambda_j \sim \frac{\varepsilon^2}{6D}\left(\frac{\int_{-\infty}^{\infty}\left[u_c(y)\right]^3\,dy}{\int_{-\infty}^{\infty}\left[u_c'(y)\right]^2\,dy}\right)\sigma_j\,, \tag{5.37}$$

where σ_j is an eigenvalue of the matrix eigenvalue problem

$$(\mathcal{R} - \mathcal{F})\,\boldsymbol{c} = \sigma \boldsymbol{c}\,. \tag{5.38a}$$

Here $\mathcal{F}$ is defined in (5.24). The matrix $\mathcal{R}$ is defined by

$$\mathcal{R} \equiv 2D^3 \mathcal{C}\mathcal{P}\left(I + D\mathcal{C}\mathcal{G}\right)^{-1} \mathcal{C}\left(\beta^{-1}\mathcal{H} - I\right)\mathcal{P}^t\,, \tag{5.38b}$$

where

$$\mathcal{H} \equiv \mathcal{K}\mathcal{C}\left(I + D\mathcal{C}\mathcal{G}\right)^{-1}\,, \qquad \mathcal{K} \equiv \boldsymbol{e}\boldsymbol{e}^t = \begin{pmatrix} 1 & \cdots & 1 \\ \vdots & \ddots & \vdots \\ 1 & \cdots & 1 \end{pmatrix}\,. \tag{5.38c}$$

The constant β in (5.38b) is defined in (5.33).

We first show that our result reduces to that obtained in [7] for the special case of a symmetric spike pattern. For a symmetric pattern $v_j = 6bk$ for $j = 1, .., k$. Thus, $\mathcal{C}$ and $\mathcal{F}$ are multiples of the identity matrix given by

$$\mathcal{C} = \frac{1}{6bDk^2} I\,, \qquad \mathcal{F} = \frac{1}{6bk} I\,. \tag{5.39}$$

Equation (5.38) then becomes

$$\left(-\frac{k}{2D} I + \gamma \mathcal{P}\left(I + \gamma\mathcal{G}\right)^{-1}\left(\beta^{-1}\mathcal{H} - I\right)\mathcal{P}^t\right)\boldsymbol{c} = \frac{3\sigma k^2 b}{D}\boldsymbol{c}\,, \tag{5.40}$$

where

$$\gamma = \frac{1}{6bk^2}\,, \qquad \mathcal{H} = \frac{\gamma}{D}\mathcal{K}\left(I + \gamma\mathcal{G}\right)^{-1}\,. \tag{5.41}$$

For a symmetric spike pattern (2.24a) becomes

$$v_e(x) \sim \frac{1}{k}\sum_{j=1}^{k} G(x; x_j) + \bar{v}\,. \tag{5.42}$$

By evaluating (5.42) at $x = x_i \equiv -1 + (2i-1)/k$, we obtain that $\boldsymbol{e}$ is an eigenvector of the matrix $\mathcal{G}$. By differentiating (5.42) at $x = x_i$, and using the equilibrium condition (5.3) that $\langle v_{ex}\rangle_i = 0$ for $i = 1, .., k$, we get that $\mathcal{P}\boldsymbol{e} = 0$, where $\mathcal{P}$ is the matrix defined in (5.35). Thus, since $\mathcal{K} = \boldsymbol{e}\boldsymbol{e}^t$, we

conclude that the matrix product $\mathcal{P}\left(I+\gamma\mathcal{G}\right)^{-1}\mathcal{H}$ in (5.40) is identically the zero matrix. Thus, for a symmetric spike pattern, (5.38) reduces to the following matrix problem considered in [7]:

$$\mathcal{M}\boldsymbol{c}=\omega\boldsymbol{c} \qquad \sigma=\frac{D}{3k^2b}\omega\,, \tag{5.43a}$$

where

$$\mathcal{M}=-\frac{k}{2D}I-\gamma\mathcal{P}\left(I+\gamma\mathcal{G}\right)^{-1}\mathcal{P}^t\,. \tag{5.43b}$$

The eigenvalues of $\mathcal{M}$ were computed explicitly in ([7]) with the result

$$\omega_1=-\frac{k}{2D}\,; \qquad \omega_j=\frac{k}{2D}\left[\frac{\left(1-\frac{\gamma}{2DK}\right)\tan^2\left(\frac{\theta_j}{2}\right)}{\tan^2\left(\frac{\theta_j}{2}\right)-\frac{\gamma}{2Dk}\sec^2\left(\frac{\theta_j}{2}\right)}\right]\,, \quad j=2,..,k\,, \tag{5.44}$$

where $\theta_j=\pi(j-1)/k$ for $j=2,..,k$. When $\gamma=2Dk$, then $\omega_j=0$ for $j=2,..k$. It is at this value that the stability of the symmetric branch s_k with respect to the small eigenvalues changes. In this way, the following result was obtained in [7]:

Proposition 5.3 (**From [7]**): *Consider a symmetric k-spike equilibrium solution where* $x_j=-1+(2j-1)/k$ *for* $j=1,..,k$. *Then, for* $\varepsilon\ll 1$, *the eigenvalues* λ *of (3.2) of order* $O(\varepsilon^2)$ *are all real, and they are all negative when*

$$D<D_m=\frac{1}{12bk^3}\,. \tag{5.45}$$

When $D>D_m$, *then* $k-1$ *small eigenvalues are positive. When* $D=D_m$, $\lambda=0$ *is an eigenvalue of algebraic multiplicity* $k-1$. *Furthermore,* $D_m<D_k$, *where* D_k, *given in (3.19) is the largest value of D for which the symmetric branch* s_k *is stable with respect to the large* $O(1)$ *eigenvalues.*

Since $D_m<D_k$, the symmetric branch s_k is stable with respect to both the large and small eigenvalues only when $D<D_m$. Notice that the critical value D_m is precisely the value of D given in Result 2.4 where the asymmetric patterns bifurcate from the symmetric solution branch s_k. Thus, as D is decreased below the bifurcation value $D=D_m$, the symmetric branch s_k becomes stable with respect to the small eigenvalues. The final question we address is to determine the stability with respect to the small eigenvalues of the $k-1$ asymmetric branches (ignoring in the counting the different possible oriented sequences of the small and large spikes) that emerge from s_k at $D=D_m$. This stability calculation using (5.38) must be done numerically.

The numerical procedure is as follows. We fix k_1, k_2, b, and a specific orientation of the large and small spikes on the interval. Since the eigenvalues depend on the product bD, we take $b=1$

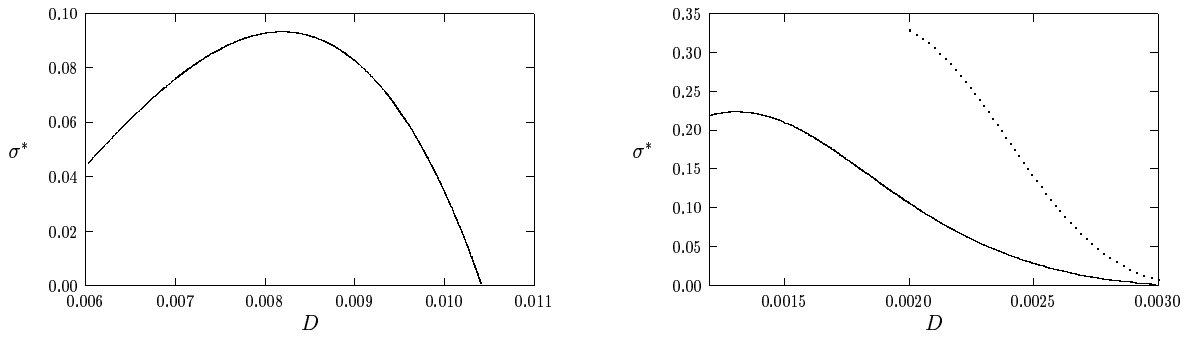

(a) AB pattern

(b) ABB and BAB patterns

Figure 10: Plot of σ^*, defined in (5.46), for two and three-spike patterns with $b = 1$. The plots are shown for the range of values of D where each pattern is stable with respect to the large eigenvalues. In Fig. 10(b) the solid curve is for an ABB pattern and the dotted curve is for a BAB pattern.

without loss of generality and we let D be a continuation parameter. We then compute z and $\tilde{z}$ from (2.14). This determines z_1,..,z_k and from this we calculate $v_j = 6b/l_j$ from (2.23b). In terms of v_j we then evaluate the matrix $\mathcal{F}$ in (5.24). In calculating the matrix $\mathcal{R}$ in (5.38b), we use the explicit formula (2.25c) for the Green's function $G(x; x_j)$. The eigenvalues σ_j of the matrix $\mathcal{R} - \mathcal{F}$ in (5.38) are calculated numerically using LAPACK [1]. The maximum eigenvalue of this matrix is denoted by

$$\sigma^* = \text{Max}(\sigma_j) \qquad \text{for} \quad j = 1, .., k\,. \tag{5.46}$$

From Proposition 5.2, we conclude that a k-spike pattern is unstable when $\sigma^* > 0$.

In Fig. 10(a) and Fig. 10(b) we plot σ^* versus D for two and three spike patterns, respectively. In each case we have plotted σ^* versus D over the range of values of D for which the pattern exists and is stable with respect to the large eigenvalues (these ranges were given in §4). In Fig. 11 we plot σ^* versus D for certain four spike patterns. In each case we have found that $\sigma^* > 0$ over this range, indicating that the asymmetric pattern is unstable with respect to the small eigenvalues. Further numerical computations (not shown) also indicate that although an asymmetric branch may be stable with respect to the large eigenvalues for some range of D, they are always unstable with respect to the small eigenvalues on this range. Unfortunately, due to the difficulty in studying the

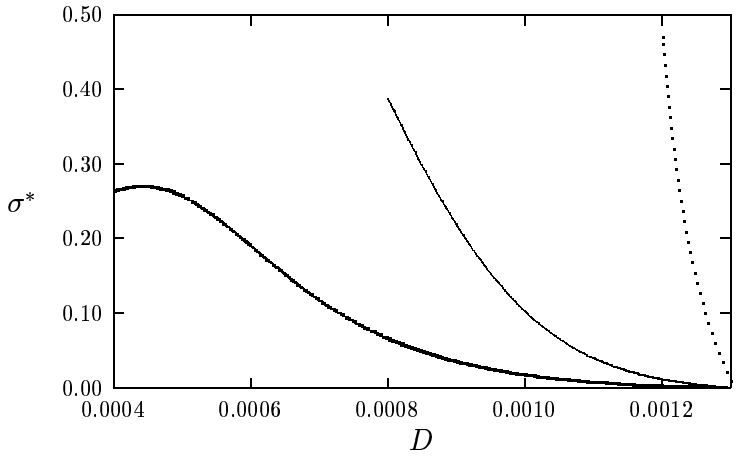

Figure 11: Plot of σ^*, defined in (5.46), for four-spike patterns with $b = 1$. The heavy solid curve is for an ABBB pattern, the solid curve is for a BABB pattern, and the dotted curve is for a BABA pattern. In each case we have plotted σ^* versus D for the range of D where the pattern is stable with respect to the large eigenvalues.

eigenvalue problem (5.38) analytically, we are not able to provide a rigorous analytical justification to confirm this numerical observation.

6 Conclusions

We have used formal asymptotic analysis to construct asymmetric equilibrium spike patterns for the Schnakenburg model, and we have analyzed the stability properties of these solutions. We have determined ranges of D for which asymmetric patterns exist, and other ranges of D where these patterns are stable with respect to temporal instabilities on a fast $O(1)$ time scale. We formulated a matrix eigenvalue problem whose eigenvalues determine the stability of the asymmetric equilibrium spike patterns on a long $O(\varepsilon^{-2})$ time scale. From numerical computations of this matrix eigenvalue problem, we show that for the ranges of D where the asymmetric patterns are stable with respect to the large $O(1)$ eigenvalues, the patterns are always unstable with respect to the small $O(\varepsilon^2)$ eigenvalues.

The analysis presented above generalizes the typical Turing analysis based on linearizing a reaction-diffusion system around a spatially homogeneous equilibrium state. A similar analysis of

asymmetric spike patterns was made for the Gierer-Meinhardt model in [16], and similar conclusions were obtained regarding the existence and the stability properties of these solutions. It is hoped that the analytical methods developed in this paper and in [16] will become a common tool for the analysis of spike-type patterns in other reaction-diffusion systems.

A Calculation of the Matrices $\mathcal{B}$ and $\mathcal{C}$

Consider the boundary value problem

$$D\eta^{''} = 0\,, \qquad \eta^{'}(\pm 1) = 0\,, \tag{A.1a}$$

$$[\eta]_j = 0\,, \qquad \left[D\eta^{'}\right]_j = \frac{6b}{v_j^2}\eta_j - \omega_j D\,, \tag{A.1b}$$

for $j = 1, \ldots, k$, where $[\eta]_j \equiv \eta(x_{j+}) - \eta(x_{j-})$ and x_j satisfies (2.27). In (A.1b), $\eta_j = \eta(x_j)$ and ω_j is defined by

$$\omega_j = -\frac{2b}{D}\int_{-\infty}^{\infty} u_c\,\phi_j\,dy\,. \tag{A.2}$$

Let $\boldsymbol{\eta}^t = (\eta_1, \ldots, \eta_k)$. To obtain a linear system for $\boldsymbol{\eta}$, we solve (A.1) analytically on each subinterval and impose the continuity of $\eta(x)$ to get

$$\eta(x) = \begin{cases} \eta_1\,, & -1 < x < x_1\,, \\ \frac{\eta_j}{d_{j+1}}(x_{j+1} - x) + \frac{\eta_{j+1}}{d_{j+1}}(x - x_j)\,, & x_j < x < x_{j+1}\,, \quad j = 1, \ldots, k-1\,, \\ \eta_k\,, & x_k < x < 1\,. \end{cases} \tag{A.3}$$

Here $d_j = x_j - x_{j-1}$. Imposing the jump conditions on $D\eta^{'}$ from (A.1b), we obtain the system of equations,

$$\frac{\eta_1}{d_2} - \frac{\eta_2}{d_2} = -\frac{6b\eta_1}{Dv_1^2} + \omega_1\,, \tag{A.4a}$$

$$-\frac{\eta_{j-1}}{d_j} + \eta_j\left(\frac{1}{d_j} + \frac{1}{d_{j+1}}\right) - \frac{\eta_{j+1}}{d_{j+1}} = -\frac{6b\eta_j}{Dv_j^2} + \omega_j\,, \qquad j = 1, .., k-1\,, \tag{A.4b}$$

$$-\frac{\eta_{k-1}}{d_k} + \frac{\eta_k}{d_k} = -\frac{6b\eta_k}{Dv_k^2} + \omega_k\,. \tag{A.4c}$$

Writing (A.4) as a linear system for $\boldsymbol{\eta}$ we obtain the matrix formulation given in (3.6) and (3.7).

Acknowledgements

M. J. W. thanks NSERC for their grant support and the Chinese University of Hong Kong for their hospitality when writing this paper. J. W. thanks the support of RGC of Hong Kong.

References

[1] E. Anderson et al. *Lapack User's Guide: Third Edition*, SIAM Publications (1999).

[2] A. Doelman, T. J. Kaper, H. van der Ploeg, *Spatially Periodic and Aperiodic Multi-Pulse Patterns in the One-Dimensional Gierer-Meinhardt Equation*, to appear, Methods Appl. Anal. (2001).

[3] A. Gierer, H. Meinhardt, *A Theory of Biological Pattern Formation*, Kybernetik, **12**, (1972), pp. 30–39.

[4] L. Harrison, D. Holloway, *Order and Localization in Reaction-Diffusion Pattern*, Physica A, **222**, (1995), pp. 210-233.

[5] A. Hunding, M. Brøns, *Bifurcation in a Spherical Reaction-Diffusion System with Imposed Gradient*, Physica D, **44**, (1990), pp. 285-302.

[6] D. Iron, M. J. Ward, J. Wei, *The Stability of Spike Solutions to the One-Dimensional Gierer-Meinhardt Model*, Physica D, **150**, No. 1-2, (2001), pp. 25-62.

[7] D. Iron, J. Wei, M. Winter, *Stability Analysis of Turing Patterns Generated by the Schnakenberg Model*, preprint, (2001).

[8] D. Iron, M. J. Ward, *The Dynamics of Multi-Spike Solutions to the One-Dimensional Gierer-Meinhardt Model*, submitted, SIAM J. Appl. Math., (2001).

[9] P. K. Maini, D. Benson, J. A. Sherratt, *Pattern Formation in Reaction-Diffusion Modles with Spatially Inhomogeneous Diffusion Coefficients*, IMA J. Math. Appl. Med. Biol., **9**, (1992), pp. 197-213.

[10] P. K. Maini, K. J. Painter, H. N. P. Chau, *Spatial pattern formation in chemical and biological systems,* Faraday Transactions, **93**, (1997), pp. 3601-3610.

[11] H. Meinhardt, *Models of Biological Pattern Formation*, Academic Press, London (1982).

[12] H. Meinhardt, *The Algorithmic Beauty of Sea Shells*, Springer (1995).

[13] M. R. Myerscough, P. K. Maini, K. J. Painter, *Pattern Formation in a Generalized Chemotactic Model*, Bull. of Math. Biol., **60**, (1998), pp. 1-26.

[14] J. Schnakenberg, *Simple Chemical Reaction Systems with Limit Cycle Behavior*, J. Theoret. Biology, **81**, (1979), p. 389-400.

[15] A. Turing, *The Chemical Basis of Morphogenesis*, Phil. Trans. Roy. Soc. B, **327**, (1952), pp. 37-72.

[16] M. J. Ward, J. Wei, *Asymmetric Spike Patterns for the One-Dimensional Gierer-Meinhardt Model*, to appear, Europ. J. Appl. Math., (2001).

[17] J. Wei, *On Single Interior Spike Solutions for the Gierer-Meinhardt System: Uniqueness and Stability Estimates*, Europ. J. Appl. Math., Vol. **10**, No. 4, (1999), pp. 353-378.

[18] J. Wei, M. Winter, *Existence and Stability Analysis of Multiple-Peaked Solutions*, preprint, (2001).